JMEPEG (2012) 21:2446–2450
DOI: 10.1007/s11665-011-0094-y

1059-9495/$19.00

Study of Interfacial Stress Distribution in SiC Fiber Reinforced Titanium Matrix Composites on Transverse Tensile Tests

Xu Yanfang, Su Tiexiong, and Yuan Meini

(Submitted August 25, 2011; in revised form November 9, 2011)

A combination of the transverse tensile test and the unilaterally coupled finite element method was used to evaluate the interfacial normal bond strength and stress distribution of titanium matrix composites (TMCs). In addition, in order to identify the interface shear failure mode of TMCs under transverse loading, both the push-out test and the finite element method have been developed to characterize the interfacial shear strength of TMCs, which is the interfacial shear failure criterion. This article studies the results of the experiments, which suggested that the interfacial normal bond and shear strength of SiC_f/Ti-6Al-4V were 300 and 350 MPa, respectively, and the interface failure mode of TMCs under the transverse tensile test was radial failure rather than shear failure. Moreover, the effect of residual stress on the radial stress is also discussed in detail in this article.

Keywords failure analysis, metal matrix composites, surface engineering

1. Introduction

For SiC fiber reinforced titanium matrix composites (TMCs), the transverse mechanical properties have to be considered. The cruciform specimen is an appropriate one to evaluate the transverse mechanical properties of TMCs (Ref 1-3). It is noted that the transverse mechanical properties of TMCs are significantly influenced by the fiber/matrix interface properties. For example, the transverse creep resistance can be improved by increasing the fiber-matrix normal bong strength. Thus, more and more attention has been paid to evaluate the interface normal bond strength of TMCs (Ref 4-6). In previous studies, a fully coupled finite element method, which could easily result in the loss of thermal residual stresses, was used to characterize the interface normal bond strength. For instance, Gundel and Miracle (Ref 6) adopted a fully coupled finite element method to evaluate the interface normal bond strength of SiC_f/Ti-6Al-4V, and the calculated value was lower than the actual value (Ref 7, 8). In addition, it is also very important to clearly identify the interface failure mechanism of TMCs under the transverse tensile test, since different interface failure modes influence seriously the different micro-stress distribution and the ductility and creep resistance of TMCs (Ref 9-11).

In this article, both the transverse tensile test and the unilaterally coupled finite element method were used to evaluate the interfacial normal bond strength and the interfacial stress distribution of TMCs. Furthermore, in order to identify the interface shear failure mode of TMCs under transverse loading, a combination of the push-out test and the finite element method has been developed to predict the interfacial shear strength of TMCs, which is the interfacial shear failure criterion.

2. Experiments

2.1 Material

SiC_f/Ti-6Al-4V was prepared in the form of foil-fiber-foil. The Textron SCS-6 SiC fiber was selected, with a radius of 0.07 mm, and the Young Modulus 469 GPa. The Ti-6Al-4V foil of 0.1 mm in thickness was manufactured through cold-rolling. The consolidation of SiC_f/Ti-6Al-4V composites was conducted by vacuum hot pressing at a temperature of 920 °C for 1 h under a pressure of 70 MPa. After hot pressing, the composite was allowed to cool in vacuum in the furnace until it was at room temperature. Then, the composite was removed from the furnace.

2.2 The Transverse Tensile Test

The specimen of the transverse tensile test (the cruciform specimen) shown in Fig. 1 was cut to approximate dimensions with electric discharge cutting. The length and width of the specimen were 50.8 and 38 mm, respectively. The transverse tensile test of SiC_f/Ti-6Al-4V was performed at room temperature on an Instron1195 electronic tensile machine at a speed of 1 mm/min. In order to obtain the precise tensile strain in the specimen center, the electric-resistance strain gauge was adhered to the cruciform specimen center. The area of the strain gauge was 1 mm^2. Figure 2 shows the transverse stress-strain behavior of SiC_f/Ti-6Al-4V. In the initial region, the

Xu Yanfang, Su Tiexiong, and **Yuan Meini**, College of Mechanical and Electrical Engineering, North University of China, Taiyuan 030051, People's Republic of China. Contact e-mail: xuyanfang1968@163.com.

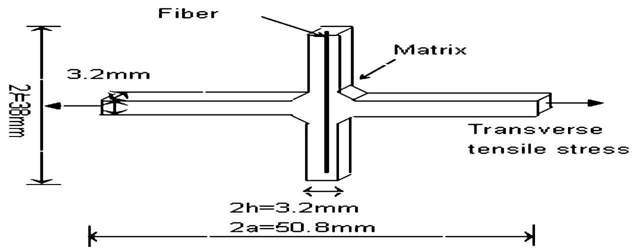

Fig. 1 Schematic of the cruciform specimen

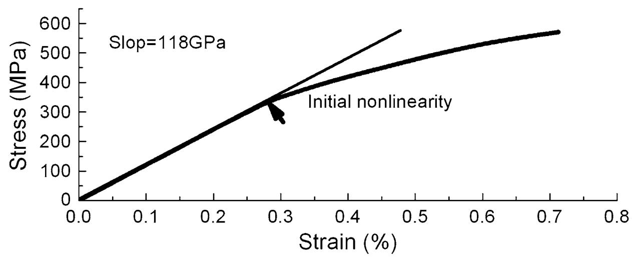

Fig. 2 The transverse stress-strain behavior of SiC_f/Ti-6Al-4V

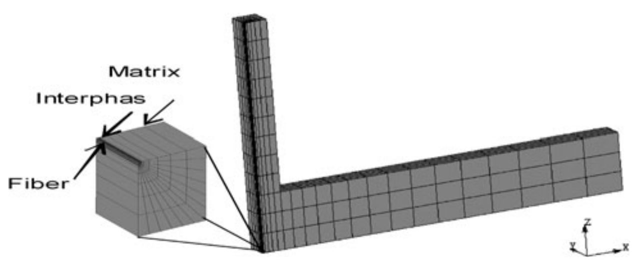

Fig. 3 Finite element model of the cruciform specimen and the enlarged region at the center

response was linear corresponding to the elastic loading of a composite with a perfectly bond interface until inflexion point occurs. At inflexion point, the stress and strain were 330 MPa and 0.26%, respectively. In the next region, the response was non-linear corresponding to progressive debonding of interface.

Next, the transverse tensile test was modeled using finite element method. In consideration of symmetry, one-eighth of the total cruciform specimen was modeled, as illustrated in Fig. 3. The fiber, the interface, and the matrix were treated as three-dimensional eight-node brick elements. SiC/Ti-6Al-4V was selected as the model material. TiC was used to represent interfacial reaction product, in that the main interfacial reaction product of TMCs is TiC, especially when SiC fiber has a pure C coating (Ref 12, 13). In finite element analysis, SiC fiber, titanium alloy matrix, and interfacial material were treated as perfectly isotropic elastic materials. Table 1 shows the variations of the thermo-mechanical properties of Ti-6Al-4V, TiC, and SiC fiber. The finite element modeling processes were described as follows.

When titanium matrix composites were cooling from high temperature to room temperature, thermal residual stresses were induced due to the mismatch of the coefficient of thermal expansion (CTE). The coefficients of thermal expansion of Ti-6Al-4V, SiC, and TiC at room temperature are 8.6×10^{-6}/°C, 4.0×10^{-6}/°C, and 7.6×10^{-6}/°C, respectively. In finite element analysis, the cooling process can be modeled using thermal load. Moreover, we assumed a reference temperature (T_{ref}) above which the composites were stress free. For SiC_f/Ti-6Al-4V composites, reference temperature is about 700 °C (Ref 14). Boundary conditions were that these axisymmetrical planes were constrained by symmetry conditions, whereas the outer surfaces were free to move in all direction. Next, the transverse tensile test was modeled, and a new finite element model was required. Thermal residual stresses computed in previous numerical simulation were introduced in the new model. Next, a face load was applied on the surface (x = 25.4 mm) of the new finite element model. Boundary conditions are the same as that of the cooling process of composites.

Table 1 Thermo-elastic parameters of SiC, TiC, and Ti-6Al-4V used in finite element analysis

Material	Temperature, °C	*E*, GPa	ν	α, $\times 10^{-6}$/°C
Ti-6Al-4V	28	105	0.23	8.6
	200	94.7	0.23	9.0
	400	84.1	0.23	9.2
	600	74.2	0.23	9.4
	800	62.8	0.24	9.5
SiC (all temperature)	All temperature	469	0.17	4.0
TiC (all temperature)	All temperature	440	0.19	7.6

2.3 The Push-Out Test

The specimen of the push-out test was cut from SiC_f/Ti-6Al-4V composites perpendicular to the fiber long axis and then ground and polished to a thickness of about 0.5 mm. The microhardness testing machine (HIT-300) was used to conduct the push-out test. The experimental procedure was that when the fiber was selected under microscope, the specimen was moved under the loaded indenter using the precision positioning system. Then the loaded flat indenter would exert pressure until the fiber was pushed out of the composite specimen completely.

Next, the push-out test was modeled by means of finite element method. An axi-symmetric cylindrical model was adopted as the finite element model, which consisted of the SiC fiber, the interface and the titanium alloy matrix, as shown in Fig. 4. The height of the model was 0.5 mm, the radii of the fiber, the interface, and the matrix were 0.07, 0.071, 0.171 mm, respectively. The elements of SiC fiber, interface, and titanium alloy matrix were isoparametric 4-noded quadrilateral elements. The finite element modeling process of the push-out test consisted of two steps: (1) Modeling the cooling process of titanium matrix composites; and (2) Modeling the push-out test process. The finite element analysis of the push-out test was described in detail elsewhere (Ref 15, 16).

3. Results and Discussion

3.1 Estimation of Interfacial Normal Bond Strength

The transverse stress-strain behavior of SiC_f/Ti-6Al-4V (Fig. 2) aforementioned showed that the initial non-linearity in the stress-strain curve occurs at transverse tensile stresses of 330 MPa. At this applied stress, the matrix of Ti-6Al-4V is far

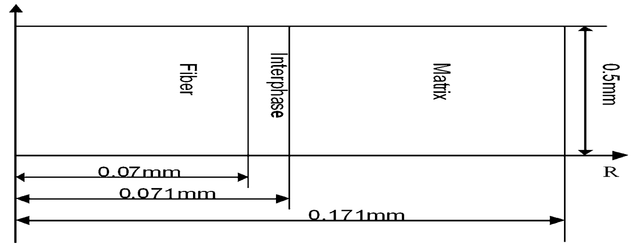

Fig. 4 Axi-symmetric finite element model of the push-out test

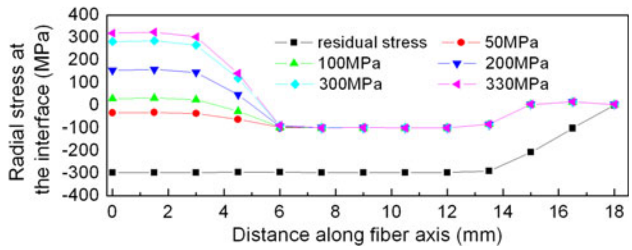

Fig. 5 The interfacial stress distribution on the *x-z* plane ($x = 0.07$ mm) as a function of distance along the fiber axis

more not yield, hence interfacial failure occurs at the specimen center. Figure 5 shows the distribution of radial stresses at the interface under different transverse tensile stresses for SiC_f/Ti-6Al-4V. According to Figure 5, when the transversely tensile stresses are 330 MPa, the radial stresses at the interface are about 300 MPa. So it can be deduced that interfacial normal strength is about 300 MPa. In the previous studies, a fully coupled method was often adopted to evaluate the interface bond strength, which would result in the loss of thermal residual stresses, therefore interfacial bond strength was estimated as 115 MPa for SiC_f/Ti-6Al-4V. In addition, the preparation process of SiC_f/Ti-6Al-4V is different.

3.2 Estimation of Interfacial Shear Strength

The push-out test of SiC_f/Ti-6Al-4V has been performed to obtain the experimental load-displacement curve, as illustrated in Fig. 6. The peak load and interfacial frictional force were 15 and 6 N, respectively. Then the push-out test of SiC_f/Ti-6Al-4V was modeled with finite element method. During finite element modeling, different interfacial shear strengths and frictional coefficients were assumed. The numerical analysis load-displacement curves are shown in Fig. 7. From Fig. 6 and 7, it can be obtained that when the interfacial shear strength and frictional coefficient are assumed to be 350 MPa and 0.2, respectively, good agreement would be found between the numerical analysis curve and the experimental one. Therefore, the interfacial shear strength of SiC_f/Ti-6Al-4V is 350 MPa. Chandra and Zeng et al. (Ref 17-19) have also adopted this method to evaluate the interface shear strength of TMCs.

3.3 Interface Failure Mechanism

According to the results of the transverse tensile test (Fig. 2), the initial non-linearity in the transverse stress-strain curve occurs at the applied stresses of 330 MPa for SiC_f/Ti-6Al-4V. Because the displacement associated with shear failure is very small, the initial non-linearity in the stress-strain curve is only resulted from interfacial radial separation at $\theta = 0°$. It can

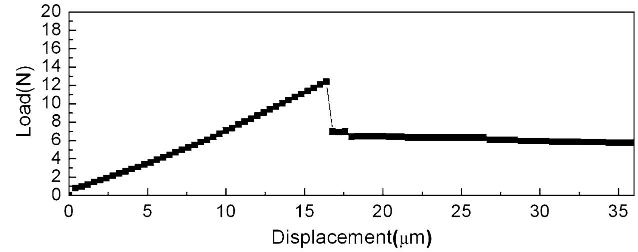

Fig. 6 The experimental load-displacement curve of SiC/Ti-6Al-4V composite

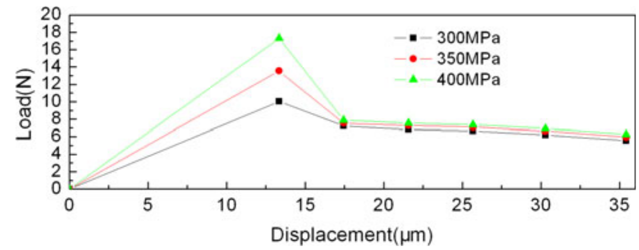

Fig. 7 The numerical analysis load-displacement curve of SiC/Ti-6Al-4V composite

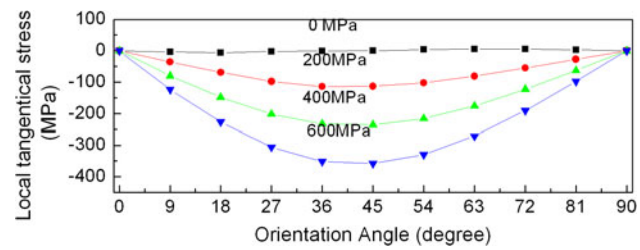

Fig. 8 Interfacial shear stress distribution as a function of the circle orientation

be concluded that when the applied stress is about 330 MPa, interface radial stresses at $\theta = 0°$ is larger than the interfacial normal bond strength, and radial interface failure occurs. However, interfacial shear failure is unknown. Finite element method was used to analyze the interfacial shear stresses distribution, as shown in Fig. 8. From Fig. 8, it can be obtained that when the applied stresses are about 400 MPa, the maximum shear stresses at $\theta = 45°$ are 240 MPa. The interface shear strength of SiC_f/Ti-6Al-4V evaluated is about 350 MPa, which is higher than the value of the maximum shear stresses. Therefore, when the applied stresses are about 400 MPa, interfacial shear failure could not occur. The fracture surfaces (shown in Fig. 9) of TMCs under transverse tensile stress are relatively smooth. This also indicates that the interface failure mode of TMCs under the transverse tensile test is only radial separation instead of shear failure.

3.4 Effect of Residual Stress on the Interfacial Radial Stress

During the modeling of the transverse loading process of composites, different test temperatures are assumed. It means that the transverse tensile test was conducted under different levels of thermal stress. Figure 10 shows interfacial thermal residual stress and radial stress ($x = 0.07$ mm) as a function of test temperature. In Fig. 10, there are two types of radial stress. One is introduced

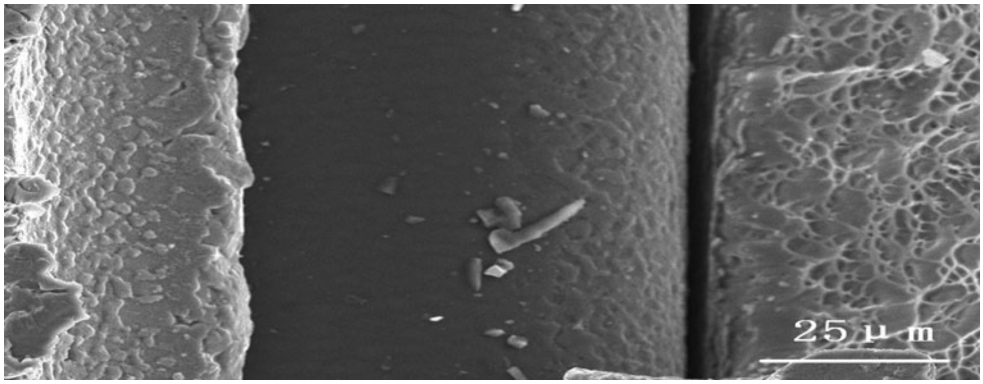

Fig. 9 SEM micrograph of TMCs fracture surface under transverse loading

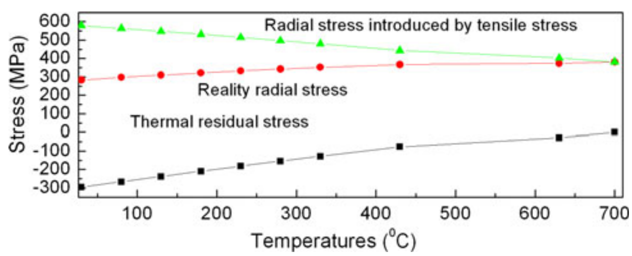

Fig. 10 Interface stress at the *x-z* plane as a function of temperature ($x = 0.07$)

from tensile stress (i.e., the applied stress), the other is resulted from thermal residual stress (i.e., the internal stress). The true radial stress in composites consists of the radial stresses introduced by tensile stress and thermal residual stress. From Fig. 10, it can be obtained that true radial stress at the interface increases with decreasing thermal residual stress (compressive). Under transverse tensile loading, the true radial stress at the fiber/matrix interface consists of mechanical stress and thermal residual stress. Mechanical stress is applied to overcome thermal residual stress, which is compressive (as shown in Fig. 5). Consequently, it is easy to understand that true radial stress at the interface would increase while thermal residual stress is decreasing.

4. Conclusions

A combination of experiments and finite element analysis is a useful method to characterize the interfacial bond strength of TMCs. Based on this method, the interfacial normal and shear strength of SiC_f/Ti-6Al-4V evaluated are 300 and 350 MPa, respectively. In addition, the interfacial stress distribution of SiC_f/Ti-6Al-4V under the transverse tensile test was obtained using finite element analysis. According to the stress distribution, we conclude that the interface failure mode of SiC_f/Ti-6Al-4V under the transverse tensile test is radial separation rather than shear failure. Besides, the true radial stress at the interface at the interface increases with decreasing in the thermal residual stress.

Acknowledgments

We would like to acknowledge the support of the Chinese Education Ministry Foundation for Doctors. Foundation item: Doctoral Fund of Ministry of Education of China (20101420120006).

References

1. J.M. Hausmann, C. Leyens, and W.A. Kaysser, Interaction Between Cyclic Loading and Residual Stresses in Titanium Matrix Composites, *J. Mater. Sci.*, 2004, **39**(2), p 501–509
2. A. Smits, D. Van Hemelrijck, T.P. Philippidis, and A. Cardon, Design of a Cruciform Specimen for Biaxial Testing of Fibre Reinforced Composite Laminates, *Compos. Sci. Technol.*, 2006, **66**(6), p 964–975
3. X.D. Wu, M. Wan, and X.B. Zhou, Biaxial Tensile Testing of Cruciform Specimen Under Complex Loading, *J. Mater. Process. Technol.*, 2005, **168**(9), p 181–183
4. D.B. Gundel, S.G. Warrier, and D.B. Miracle, The transverse Tensile Behavior of SiC-Fiber/Ti–6Al–4V Composites. Stress Distribution and Interface Failure, *Compos. Sci. Technol.*, 1999, **59**(55), p 1087–1096
5. D.B. Gundel, S.G. Warrier, and D.B. Miracle, The Interface Debond Stress in Single and Multiple SiC Fiber/Ti-6Al-4V Composites Under Transverse Tension, *Acta Mater.*, 1997, **45**(45), p 1275–1284
6. D.B. Gundel and D.B. Miracle, The Influence of Interface Structure and Composition on the Response of Single-Fiber SiC/Ti-6Al-4V Composites to Transverse Tension, *Appl. Compos. Mater.*, 1998, **5**(2), p 95–108
7. D.B. Miracle and B.S. Majumdar, Transverse Creep of SiC/Ti-6Al-4V Fiber-Reinforced Metal Matrix Composites, *Metall. Mater. Trans. A*, 1999, **30**(2), p 301–306
8. M.M. Afahdamm, M. Pavier, and J. Smithd, Micro-Mechanics of Off-Axis Loading of Metal Matrix Composites Using Finite Element Analysis, *Int. J. Solids Struct.*, 2001, **38**, p 3905–3925
9. H. Ismar, F. Schroter, and F. Strckcher, Effects of Interfacial Debonding on the Transverse Loading Behaviors of Continuous Fibre-Reinforced Metal Matrix Composites, *Compos. Struct.*, 2001, **79**, p 1713–1722
10. M. Dong and S. Schmauder, Transverse Mechanical Behaviour of Fiber Reinforced Composites FE Modelling With Embedded Cell Models, *Compos. Mater. Sci.*, 1996, **5**, p 53–66
11. Y.Q. Yang and H.J. Dudek, Interface Stability in SCS-6 SiC/Super α2 Composites, *Scripta Mater.*, 1997, **37**, p 503–510
12. Y.Q. Yang, H.J. Dudek, and J. Kumpfert, Interfacial Reaction and Stability of SCS-6 SiC/Ti–25Al–10NB–3V–1MO Composites, *Mater. Sci. Eng. A*, 1998, **246**, p 213–220
13. S.G. Warrier, B.S. Majumdar, D.B. Gundel, and D.B. Miracle, Implications of Tangential Shear Stress Induced Failure During Transverse Loading of SiC/Ti-6Al-4V Composites, *Acta Mater.*, 1997, **45**, p 3469–3480
14. M.N. Yuan and Y.Q. Yang, Analysis of Interfacial Behavior in Titanium Matrix Composites by Using the Finite Element Method (SCS-6/Ti55), *Scripta Mater.*, 2007, **56**, p 533–536
15. X. Wu, C. Cooper, and P. Bowen, In-situ Observations of Titanium Metal-Matrix Composites Under Transverse Tensile Loading, *Metall. Mater. Trans. A*, 2001, **32A**(7), p 1851–1860

16. M.N. Yuan, Y.Q. Yang, and H.J. Luo, Evaluation of Interfacial Properties in SiC Fiber Reinforced Titanium Matrix Composites Using an Improved Finite Element Model, *Mater. Charact.*, 2008, **59**, p 1684–1689
17. N. Chandra and C.R. Ananth, Analysis of Interfacial Behavior in MMCs and IMCs by the Use of Thin-Slice Push-Out Tests, *Compos. Sci. Technol.*, 1995, **54**, p 87–100
18. C.R. Ananth and N. Chandra, Elevated Temperature Interfacial Behaviour of MMCs: A Computational Study, *Composites A*, 1996, **27**, p 805–811
19. W.D. Zeng, P.W.M. Peters, and Y. Tanaka, Interfacial Bond Strength and Fracture Energy at Room and Elevated Temperature in Titanium Matrix Composites, *Composites A*, 2002, **33**, p 1159–1170